*Optical and Quantum Electronics* **33:** 899–906, 2001.



# Ultrafast all-optical demultiplexer based on monolithic Mach–Zehnder interferometer with integrated semiconductor optical amplifiers

M. DÜLK[1], ST. FISCHER[1*], M. BITTER[1], M. CARACCIA[1], W. VOGT[1], E. GINI[1], H. MELCHIOR[1], W. HUNZIKER[2], A. BUXENS[3], H.N. POULSEN[3] AND A.T. CLAUSEN[3]
[1]*Swiss Federal Institute of Technology, CH-8093 Zurich, Switzerland*
[2]*Opto Speed SA, CH-6805 Mezzovico, Switzerland*
[3]*Technical University of Denmark, DK-2800 Lyngby, Denmark*
*(*author for corrrespondence: E-mail: fischer@iqe.phys.ethz.ch)*

Received 30 August 2000; accepted 6 November 2000

**Abstract.** A monolithically integrated and fully packaged Mach–Zehnder interferometer with semiconductor optical amplifiers (MZI-SOA) is demonstrated as polarisation-independent high-speed demultiplexer for up to 160 Gbit/s optical time division multiplexed (OTDM) data streams.

**Key words:** Mach–Zehnder interferometer, demultiplexer

## 1. Introduction

Fiber-optical telecommunication is experiencing a phenomenal interest and excitement due to the immense growth of data traffic in our so-called information age. Optical fibers offer the intrinsic bandwidth to satisfy the demand for more and more transmission capacity. To take full advantage of this bandwidth, several multiplexing techniques are used. One of them is wavelength division multiplexing (WDM), in which different wavelengths are used for the different simultaneously transmitted channels. To further increase the capacity per fiber, electrical time division multiplexing (TDM) can be performed by temporally interleaving different channels. This leads to a higher base rate of about 10 Gbit/s per wavelength. For base rates beyond 10 Gbit/s the electrical approach of TDM becomes increasingly difficult. Hence, optical time division multiplexing (OTDM) has been introduced in order to further boost the throughput per fiber. In this scheme, the different optical channels with the same bit rate and the same wavelength are temporally interleaved to form a high-bit rate data stream, as shown in Fig. 1.

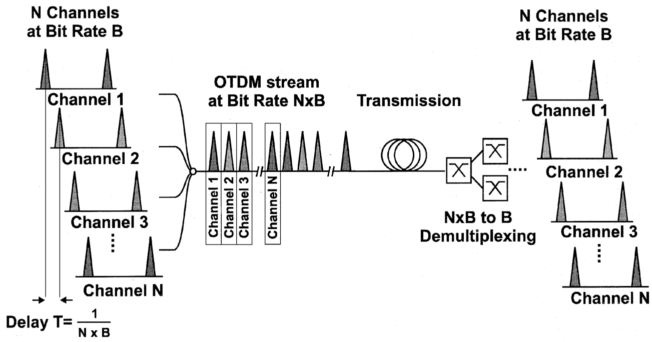


Fig. 1. One of the approaches to increase the transmission capacity per fiber is optical time division multiplexing (OTDM).

In several experiments, OTDM has already been realized for data rates of up to 160 Gbit/s per wavelength channel (Kawanishi *et al.* 1999; Mikkelsen *et al.* 1999). Consequently, optical signal processing devices like add/drop multiplexer or demultiplexer are requested to process these data rates. The demultiplexing process has to extract one low-speed channel of the high-speed OTDM stream, which can be handled by electronics. For further signal processing, the dropped channel must be in a good shape and the unwanted channels must be properly suppressed to avoid interference noise. To dissect an OTDM stream to all its different low-speed channels, this process must either be cascaded, like demonstrated in Fig. 1, or has to be done in a more sophisticated approach, as demonstrated in Fischer *et al.* (1999).

Demultiplexing at 40 Gbit/s has been achieved using two concatenated $LiNbO_3$ modulators electrically driven by the clock signal (Ellis *et al.* 1993) or with an all-optical MZI-SOA in Hess *et al.* (1998a). A single electro-absorption modulator (EAM) has been demonstrated to process demultiplexing of up to 80 Gbit/s (Moodie *et al.* 1995). The same data rate has also been all-optically processed with the MZI-SOA (Hess *et al.* 1998b). By cross-phase modulation of an optical fiber loop mirror, 160:10 Gbit/s demultiplexing has been achieved (Suzuki *et al.* 1994). In Mikkelsen *et al.* (1999), two concatenated EAMs were used for this high-speed process. Recently, 168:10.5 Gbit/s (Tajima *et al.* 2000) and 160:10 Gbit/s (Diez *et al.* 2000) demultiplexing has been performed with hybrid-integrated Mach–Zehnder interferometers.

Here, we present all-optical 160:10 Gbit/s demultiplexing using a polarisation-insensitive, monolithically integrated MZI-SOA module. For completeness, we also show the dropping of one 10 Gbit/s channel out of 40 and 80 Gbit/s data streams, performed with the same module.

## 2. Operational principle of the Mach–Zehnder interferometer

The MZI-SOA is a polarisation-independent active-passive InGaAsP/InP waveguide interferometer structure with monolithically integrated 500 μm long SOAs in each arm (Fischer *et al.* 1999). Two optical control pulses, that have a small delay with respect to each other, drive the MZI-SOA (Tajima 1993) as shown in Fig. 2. Each pulse induces a phase shift in the SOA of one interferometer arm. Two subsequent control pulses thereby switch the input signal from one output port to the other and back again. With this switching gate channels can be dropped out of an high-speed OTDM data stream as has already been shown with unpacked devices for 40:10 Gbit/s (Hess *et al.* 1998a) and 80:10 Gbit/s demultiplexing (Hess *et al.* 1998b).

## 3. Switching speed of the Mach–Zehnder interferometer

To assess the switching speed of the MZI-SOA, a pump-probe experiment has been carried out. A Ti:Sapphire laser pumped an optical parametric oscillator (OPO) that generated 400 fs FWHM optical pulses at a repetition rate of 80 MHz. The wavelength was set to 1550 nm. A low power probe was taken from these pulses by a beam splitter and chopped for lock-in detection. The strong remainder was split to form the two driving signals for the MZI-SOA (pump). The weak probe pulse was then sampling the gating of the MZI-SOA induced by the two control pulses. As shown in Fig. 3, a narrow switching gate of 1 ps FWHM has been achieved. The switching gate demonstrates an extinction of at least 15 dB at 3.125 ps from the center (bit interval of 320 Gbit/s). This demonstrates that the MZI-SOAs have sufficient

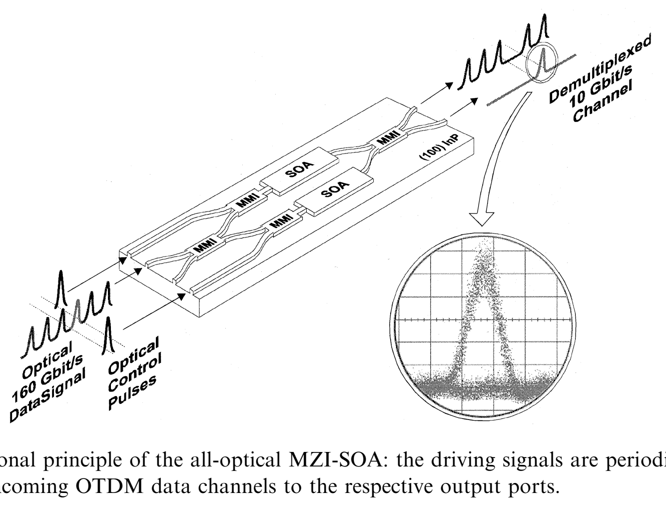


Fig. 2. Operational principle of the all-optical MZI-SOA: the driving signals are periodic control pulses switching the incoming OTDM data channels to the respective output ports.

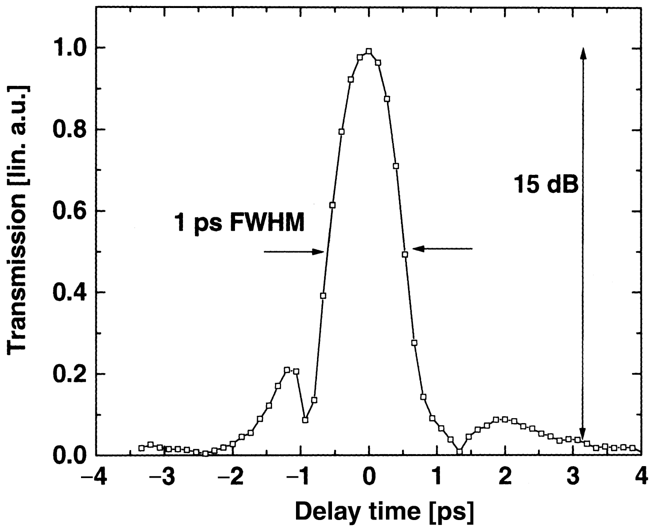


Fig. 3. Switching window measured with pump-probe technique (before deconvolution).

speed and suppression for demultiplexing operation of up to 320:10 Gbit/s. The switching energy was 280 fJ in the SOAs, bias currents were about 250 mA each.

## 4. High-bit rate demultiplexing

The setup shown in Fig. 4 was used for the 160:10 Gbit/s demultiplexing experiments. A 10 GHz gain-switched distributed feedback (GS-DFB) laser at 1553 nm generated 5 ps FWHM pulses with 20 dB extinction after a linear compression stage with dispersion compensating fiber (DCF). These pulses

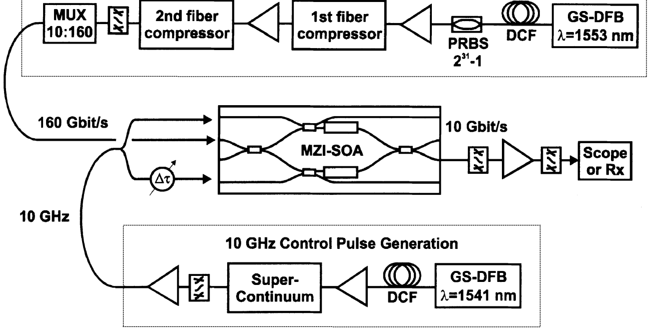


Fig. 4. Setup for the 160:10 Gbit/s demultiplexing experiment.

were externally modulated with a $2^{31} - 1$ long pseudorandom bit sequence (PRBS). A double-stage fiber compressor compressed these pulses further down to 1.5 ps FWHM. The compression mechanism is related to a fundamental property of higher-order solitons generated in the fiber due to self-phase modulation together with anomalous dispersion. These solitons follow a periodic evolution pattern such that they go through an initial narrowing phase at the beginning of each period (Zakharov and Shabet 1972). By an appropriate choice of the fiber length pulse compression can be performed (Qian and Quist 1999). The compressed 10 Gbit/s data stream was then passively multiplexed to 160 Gbit/s by four fiber multiplexers. Since each multiplexer is reducing the extinction ratio of a signal with background noise by $-3$ dB the overall extinction ratio ER of the 160 Gbit/s signal after the double-stage compressor and several amplifiers was only 4 dB. According to $\delta = 10 \cdot \log[(\mathrm{ER} + 1)/(\mathrm{ER} - 1)]$ (Agarwal 1997), the extinction ratio ER alone leads to an intrinsic power penalty $\delta$ of about 4 dB compared to the back-to-back measurement. The autocorrelation trace of the 160 Gbit/s signal is shown in Fig. 5 emphasizing the poor quality of the input stream. Due to the high amplified spontaneous emission level and the fact that the autocorrelation has been done with data instead of regular pulse streams the real pulse duration had to be derived by a fitting program taking all that into account.

For the 10 GHz control pulses, a second GS-DFB laser at 1541 nm was used. The 5 ps FWHM pulses after a DCF were launched into a fiber compressor to generate super-continuum pulses through a combination of self-phase modulation, cross-phase modulation, stimulated Raman scattering and four-wave mixing (Morioka *et al.* 1994). After an optical bandpass filter of 1.3 nm bandwidth, 2.0 ps FWHM pulses with an extinction better than 20 dB were obtained. These pulses were amplified and split to form the consecutive driving signals for the MZI-SOA. The 160 Gbit/s signal with an

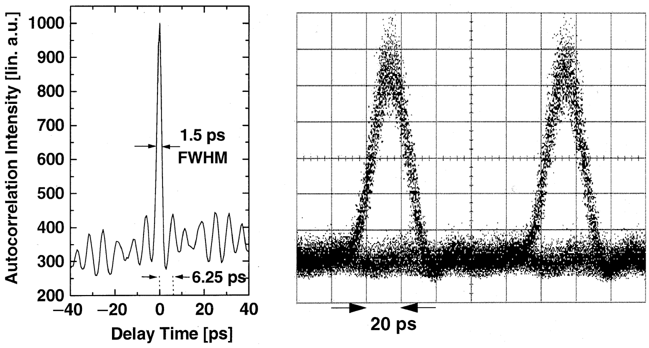


Fig. 5. Autocorrelation of 160 Gbit/s input stream (left) and eye diagram of the 160:10 Gbit/s demultiplexed channel measured with 30 GHz photodiode (right).

average power of 3 dBm was co-propagating to the 10 GHz control signal to allow for sufficient switching speed (Bishoff *et al.*, this issue).

The demultiplexed 10 Gbit/s output channel of the MZI-SOA was sent to a 30 GHz photodiode at a 50 GHz sampling head of a scope. The eye diagram shown in Fig. 5 represent therefore not the right pulse width because of the limiting 12 ps response of the photodiode. Nevertheless, it demonstrates that the eyes are open and the neighboring timing channels of the 160 Gbit/s data stream are well suppressed by the MZI-SOA demultiplexer. However, the insufficient extinction ratio of the 160 Gbit/s data signal did not allow error-free operation shifting the needed optical power into the maximum limit of the receiver. The best reachable bit error rate (BER) was $2 \times 10^{-5}$ at an optical power of $-20$ dBm at the pre-amplified receiver. In a future experiment, by using an input signal with higher quality, we expect to reach error free operation.

## 5. Lower-speed demultiplexing

For further characterization of the MZI-SOA, demultiplexing experiments at 40 and 80 Gbit/s have been performed. To get an improved switching, broader pulses are needed (Bishoff *et al.*, this issue), which can be realized by changing the setup of Fig. 4 as follows.

For the 40:10 Gbit/s experiment, the pulse widths for control and data signal were in the order of 5 ps FWHM for both by skipping all compressor units. Furthermore, only two fiber multiplexers were used to obtain the 40 Gbit/s PRBS data stream which means an improvement of at least 6 dB in the ER compared to the 160 Gbit/s case. The results are shown in Fig. 6

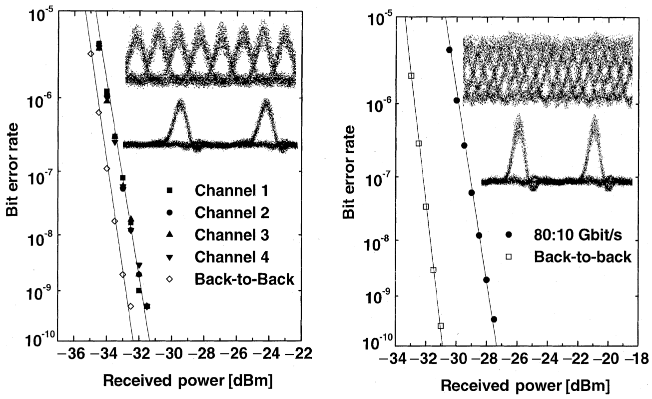


Fig. 6. Bit error rate (BER) results of the 40:10 Gbit/s (left) and 80:10 Gbit/s (right) demultiplexing experiments. The insets show the eye diagrams of the corresponding input signals with the dropped 10 Gbit/s channels below (recorded with a 30 GHz photodiode).

demonstrating a low penalty of less than 1 dB for all four 10 Gbit/s channels. Due to the polarisation-independent device design the influence of the input signal polarisation on the BER is below 1 dB. The channel selection has been done by adjusting the electrical delay of the driving signal for the control pulse source.

For the 80:10 Gbit/s demultiplexing, the pulse widths were adjusted to 3.0 ps FWHM for the control pulses by tuning the filter at the output of the super-continuum generator, and 2.2 ps FWHM for the 80 Gbit/s signal by using only the first of the two compressors shown in Fig. 4. The results are also shown in Fig. 6. The power penalty is 3.5 dB for the dropped channels compared to the 10 Gbit/s back-to-back measurement.

## 6. Ability for add/drop multiplexing

Using the discussed approach for switching, add/drop multiplexing can be achieved by optimizing for both output ports of the MZI-SOA. Thus, we get the dropped 10 Gbit/s channels as well as the remaining $3 \times 10$ Gbit/s channels or the $7 \times 10$ Gbit/s with the drawback of not optimized dropping performance (Hess *et al.* 1998a). The corresponding remaining channels are shown in Fig. 7. Due to the strong control pulses inducing the dropping process, the SOA gains are periodically saturated. The temporal gain recovery is influencing the following channels differently, which can be seen in the varying amplitudes. This recovery effect is limiting the add/drop multiplexing functionality of this approach. A more sophisticated solution for add/drop multiplexing has been presented in Fischer (2000).

## 7. Conclusions

Optical time division multiplexing (OTDM) is one of the techniques which allow to increase the transmission capacity per fiber. To be able to process the resulting high-bit rate data streams, high-speed optical demultiplexers

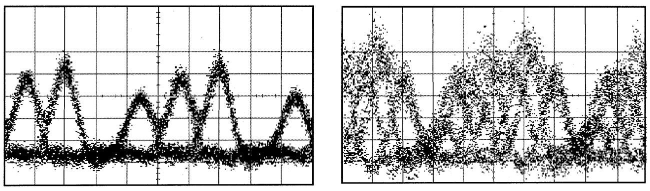

Fig. 7. Remaining $3 \times 10$ Gbit/s (left) and $7 \times 10$ Gbit/s (right) traces indicating pattern effects because of gain saturation after the strong control pulses (horizontal axis: 20 ps/div).

and add/drop multiplexers will be required in these networks. A promising candidate for these tasks is the all-optical polarisation-independent Mach–Zehnder interferometer with monolithically integrated semiconductor optical amplifiers. Demultiplexing experiments from 40:10, 80:10 and 160:10 Gbit/s have been employed to demonstrate the functionality of the device for future high-speed OTDM systems. Switching gates of 1 ps FWHM duration and extinction ratio of 15 dB prove the ability for processing even higher data rates, whereas the problem shifts to the generation of short and high-quality pulses. Add/drop multiplexing can be performed with this approach but pattern effects bring on the demand for a better solution, for example as presented in Fischer (2000). The device is fully packaged into a stable and robust module which enables the applicability in real network environments.

## References


Agrawal, G.P., *Fiber-Optic Communication Systems*, Wiley, 1997.

Bishoff, S., A. Buxens, St. Fischer, M. Dülk, A.T. Clausen, H.N. Poulsen and J. Mrk. (submitted to this special issue of *Optical and Quantum Electronics*).

Diez, S., C. Schubert, R. Ludwig, H.-J. Ehrke, U. Feiste, C. Schmidt and H.G. Weber. *Electron. Lett.* **36** 1484, 2000.

Ellis, A.D., T. Widdowson, X. Shan, G.E. Wickens and D.M. Spirit. *Electron. Lett.* **29** 990, 1993.

St. Fischer, M. Dülk, E. Gamper, W. Vogt, E. Gini, W. Hunziker, H. Melchior, A. Buxens, H.N. Poulsen and A.T. Clausen. *IEEE Photon. Techn. Lett.* **12** 335, 2000.

St. Fischer, M. Dülk, M. Puleo, R. Girardi, E. Gamper, W. Vogt, E. Gini, W. Hunziker and H. Melchior. *IEEE Photon. Techn. Lett.* **11** 1262, 1999.

Hess, R., M. Caraccia, W. Vogt, E. Gamper, P.A. Besse, M. Duelk, E. Gini, H. Melchior, B. Mikkelsen, M. Vaa, K.S. Jepsen, K.E. Stubkjaer and S. Bouchoule. *IEEE Photon. Technol. Lett.* **10** 165, 1998.

Hess, R., M. Duelk, W. Vogt, E. Gamper, E. Gini, P.A. Besse, H. Melchior, K.S. Jepsen, B. Mikkelsen, M. Vaa, H.N. Poulsen, A.T. Clausen, K.E. Stubkjaer, S. Bouchoule and F. Devaux. *Electron. Lett.* **34** 579, 1998.

Kawanishi, S., H. Takara, K. Uchiyama, I. Shake and K. Mori. *Conference Proc. of Optical Fiber Communication OFC '99*, paper PD1, San Diego, USA, 1999.

Mikkelsen, B., G. Raybon, R.-J. Essiambre, K. Dreyer, Y. Su, L.E. Nelson, J.E. Johnson, G. Shtengel, A. Bond, D.G. Moodie and A.D. Ellis. *Proc. of European Conference on Optical Communications ECOC '99*, paper PD2-3, Nice, France, 1999.

Moodie, D.G., A.D. Ellis, A.R. Thurlow, M.J. Harlow, I.F. Lealman, S.D. Perrin, L.J. Rivers and M.J. Robertson. *Electron. Lett.* **31** 1370, 1995.

Morioka, T., S. Kawanishi, K. Mori and M. Saruwatari. *Electron. Lett.* **30** 1166, 1994.

Qian, Y. and S. Quist. *Proc. of European Conference on Optical Communications ECOC '99*, p. 342. Nice, France, 1999.

Suzuki, K., K. Iwatsuki, S. Nishi and M. Saruwatari. *Electron. Lett.* **30** 660, 1994.

Tajima, K., *Jpn. J. Appl. Phys.* **32/2** 1746, 1993.

Tajima, K., S. Nakamura, Y. Ueno, J. Sasaki, T. Sugimoto, T. Kato, T. Shimoda, H. Hatakeyama, T. Tamanuki and T. Sasaki. *IEICE Trans. Electron.* **E83-C** 959, 2000.

Zakharov, V.E. and A.B. Shabet. *Sov. Phys. JETP* **34** 62, 1972.